

Missing Argo Float Profiles in Highly Stratified Waters of the Amazon River Plume

GILLES REVERDIN,^a LÉA OLIVIER,^a CÉCILE CABANES,^b JACQUELINE BOUTIN,^a CLOVIS THOUVENIN-MASSON,^a
 JEAN-LUC VERGELY,^c NICOLAS KOŁODZIEJCZYK,^b VIRGINIE THIERRY,^b DMITRY KHVOROSTYANOV,^a
 AND JULIEN JOUANNO^d

^a LOCEAN, SU/CNRS/IRD/MNHN, Paris, France

^b LOPS, Brest University/CNRS/IRD/IFREMER, Plouzané, France

^c ACRI-ST, Guyancourt, France

^d LEGOS, UPS/CNRS/IRD/CNES, Toulouse, France

(Manuscript received 17 May 2023, in final form 9 November 2023, accepted 1 February 2024)

ABSTRACT: In the western tropical Atlantic Ocean close to the Amazon plume, a large loss rate of Argo-float profiles took place, that is, instances of profiles that should have happened but were not transmitted. We find that APEX and SOLO floats were not ascending to the surface in the presence of low surface practical salinity, typically on the order of 32.5 or less, because of limitations on the surface buoyancy range for those floats. This results in an overall loss of profiles from these floats that is on the order of 6% averaged over the year, with a peak of 12% in July. We also find aborted descents/incorrect grounding detections for ARVOR/PROVOR floats when surface salinity is low and the descending float reaches a strong halocline (2.6% of all the profiles in the June–August season). Altogether, the whole Argo set includes a maximum loss rate of roughly 6% in July. We find a pattern of loss that fits the surface salinity seasonal cycle and the occurrence of low surface salinity investigated from a high-resolution daily satellite salinity product in 2010–21. The agreement is even better when considering surface density instead of surface salinity, with the temperature contribution to density inducing a shift in the maximum occurrence of these events by 1 month relative to the cycle of very low salinity events. Because of changes in the float technology, the loss rate that targets the lowest surface salinities was very large until 2010, with an overall decrease afterward.

SIGNIFICANCE STATEMENT: In the western tropical Atlantic Ocean, some Argo floats were not able to ascend or descend with very low surface salinity, because of buoyancy limitations for some float types and false bottom detection on others. In this region, for surface practical salinity smaller than 32.5, this resulted in a loss of close to one-half of the Argo profiles during the last 20 years. Altogether, this undersampling of the lowest surface salinities by Argo floats modifies the upper-ocean salinity seasonal cycle, as well as longer-term trends portrayed in Argo data-based products. Furthermore, in this region, care must be taken when validating satellite salinity data with Argo data or when adjusting satellite sea surface salinity data to in situ data products.

KEYWORDS: Oceanic profilers; Mixed layer; Surface layer; Hydrologic cycle

1. Introduction

Argo profiling floats provided qualified near-real-time and delayed mode temperature and salinity profiles in the upper 2000 m for over 20 years. They currently supply the core observations for monitoring heat and freshwater contents in the ice-free oceans away from the shelves (Le Traon 2013; Roemmich et al. 2019; von Shuckmann et al. 2020; Llovel et al. 2019). The hypothesis done to map temperature and salinity in products routinely used to investigate ocean variability (Roemmich and Gilson 2009; Ishii et al. 2006; Gaillard et al. 2016; Good et al. 2013) is that Argo provides random unbiased observations. Nonetheless, in addition to an inhomogeneous observations distribution related to ocean circulation horizontal divergence or surface and near-surface drifts of the floats, questions have been raised on the propensity of the floats to fully monitor the upper-ocean freshwater (salinity) content.

This happens, either because of errors in the salinity measurement, because floats do not always sample close enough to the sea surface, or because floats might not profile when there is a particularly low surface density, due to constraints on the surface density range reachable to Argo floats when profiling up from the deep ocean (Riser et al. 2018).

The first issue has been widely documented (Böhme and Send 2005; Owens and Wong 2009; Cabanes et al. 2016; Wong et al. 2020). It involves detecting possible sensor drifts or faulty conductivity cells. Algorithms to correct sensor drifts have been widely implemented, at least in delayed mode, and assume that the correction based mostly on deep data, is also valid near the sea surface. In highly productive or particle-laden water, there is the possibility of deposits in the cell when the float gets close to the sea surface that would result in a too low near-surface salinity measurement, but this is unlikely to be a large effect with pumped CTDs used for a large part of the Argo floats, except for some early models.

The second issue is related to the presence of salinity stratification near the surface, in particular in areas of strong surface freshwater input, such as from intense rainfall, river inflow, or

Corresponding author: Gilles Reverdin, gilles.reverdin@locean.ipsl.fr

sea ice melt, which might not be properly sampled by the Argo floats. Indeed, early on, Argo floats measured salinity S only up to a level 5–7 m below the sea surface, although this progressively evolved with floats now usually measuring up to 1 or 2 m from the surface (all salinities reported in the paper are defined according to the Practical Salinity Scale of 1978; UNESCO 1981, 1983). Nonetheless, in areas where salinity stratification is large close to sea surface, this partial lack of near-surface sampling might induce biases in surface products, depending on how the subsurface measurements are extrapolated to the sea surface (Drucker and Riser 2014; Anderson and Riser 2014). This has been discussed in the context of interpreting and validating surface salinity estimated from band-L radiometric satellite missions (Boutin et al. 2016).

The issue addressed in this paper is the third one, that is, profilers not reporting a profile. Due to their design and buoyancy characteristics, Argo floats can only explore a certain range of floatability during their profiling. This is often preset by ballasting when preparing the floats for deployment (Riser et al. 2018). There are also software issues that may prevent the profile to be acquired if the vertical velocity of the float is too slow and/or the float takes too long to profile. Thus, regions of particularly low surface water density relative to density in the deeper part of the Argo float profiles are expected to present unusually large data and profile losses. We will explore in the northwestern tropical Atlantic the possibility that the float profiling and reporting capacity is hindered when the density contrast between the deep part of the profile and the surface is too large, or that there is a strong sudden vertical gradient of water density in the presence of surface fresh pools.

The northwestern tropical Atlantic Ocean region off the South American shelves in the vicinity of the Amazon plume is an appropriate region to check whether a loss of profiles related to density gradients happens. Very fresh pools of surface water have long been known to spread offshore in this region with a strong seasonality (Coles et al. 2013), peaking from May to October. Except in boreal winter, this fresher surface water is usually very warm and thus has very low surface density. Even during the expected “dry/salty” season, in February, relatively fresh water ($S < 32$) was observed crossing the shelf break near 7°N that originates from the Amazon and Para River discharge near the equator (Reverdin et al. 2021; Olivier et al. 2022). More recently, in August–September 2021, patches of very fresh surface water have been observed spreading to the northwest on the western side of an anticyclonic ring near 7°–10°N. Minimal surface salinity was as low as 24, even after separation from the shelf (Olivier et al. 2024, manuscript submitted to *Remote Sens. Environ.*). There were two Argo floats in the very fresh patches during this period, but none of the expected profiles were fully collected or transmitted. Other events with very low salinity in the same season are documented in Reul et al. (2009), but do not seem to be documented in the early Argo data.

In this region, we will evaluate how many Argo profiles are missing, that is, profiles that were not transmitted, as identified by available profile numbers, or that only include a couple of data points. We will then compare the temporal and spatial distributions of missing profiles with statistics of daily surface salinity and density from satellite products in 2010–21.

We will also evaluate the effect missing profiles with low surface salinity have on in situ data mapped surface salinity products.

2. Data

a. Argo data

The Argo float profiles used in this study are extracted from the Global Data Assembly Center (GDAC) monthly snapshot of June 2022 and originate from different models of floats since the start of the Argo program in 2000. In this region (45°–65°W, 5°S–15°N), of a total of close to 10 000 profiles, the float models are (corresponding Argo float type numbers in first set of parentheses, followed by the corresponding percentage of all the profiles) APEX floats (845 and 846) (~13.5%), SOLO floats (851 and 852) (~20%), S2A (854) and ALTO floats (873) (33.5%), ARVOR (844) and PROVOR floats (836 and 841) (~31%), as well as a few NOVA floats (865) (~2%). The ones deployed early in the program (roughly until 2011) tended to have a 5-dbar vertical resolution near the surface, with top level near 4 dbar or deeper for APEX floats, 5 dbar for SOLO floats, and 6 dbar for ARVOR/PROVOR floats (for APEX floats, these usually were discrete values, whereas for the other float types, the reported values usually were bin averages). More recent deployments tend to have higher (typically 1 dbar) resolution near the surface and end up closer to the sea surface (1 m for S2A floats and 3 m for ARVOR/PROVOR floats). S2A floats appeared in this region around 2013, and the last occurrences of SOLO profiles were in 2016, with a very small number of APEX profiles since then.

All float profiles have been quality controlled in real time, and most in delayed mode, except for the last couple of years. Often (except for S2A floats), there is a large number of uppermost salinity flagged as bad, but most commonly the flagging is also applied for a larger part of the profile (this is particularly the case for ARVOR floats, with more than 10% of flagged data). When eliminating profiles with a large part flagged as bad, we have less than 0.4% of all profiles flagged as bad only near the sea surface. Among those, for ARVOR/PROVOR floats as well as some for SOLO floats, the flagged near-surface salinity is usually low (less than 35 pss-75). Those flagged low surface salinities correspond to at most 0.4% of all ARVOR/PROVOR profiles in June–August. This “bad” flag is probably motivated by the possibility of large fouling near the surface in particle-laden Amazon plume water, but this could also correspond to real fresh pools with data incorrectly flagged as bad. However, for our study, whether this flagging is appropriately applied is a minor issue that will not be discussed further. Nonetheless, in the reported statistics, we will include either only data with “good” validated quality control (QC) flags, or alternatively include data with all QC flags (later on QC flag will be shortened as QC).

Floats perform successively numbered cycles usually including a descent to a parking depth, a drift period, followed by a descent to profile depth and an ascent with data collection to the sea surface, where the float profile is transmitted. The floats move up and down by adjustment of their buoyancy, usually by filling up an external bladder with oil or emptying

it, the oil then being stored inside the float. This can be done progressively to try to maintain a nearly constant vertical velocity, or done at once or at regular time intervals, as for the ascent of some of the SOLO floats. The vertical velocity is then mostly a function of the floatability contrast between the float and the water. Near the sea surface, the vertical velocity strongly diminishes when the water density is particularly low. Due mostly to a small bladder volume, the early APEX and SOLO floats (for SOLO, major manufacturing changes occurred around 2011–12) had a relatively small range of density that they could explore through their profile and that had to be individually set by appropriate ballasting before the deployment [see explanation for recent APEX models in [Riser et al. \(2018\)](#), which also mostly holds for earlier models]. For the SOLO floats there was also a set time for the upward profile and following surface transmission. In the presence of a strong water density contrast (very low surface density), the upward travel time can be longer with the risk of not reaching the surface in the targeted time or with not enough surface time for the transmission of the upward profile data (J. Gilson 2023, personal communication). In the case of the descent from the surface of ARVOR and PROVOR floats, if the vertical velocity remains too small despite attempts to decrease its floatability (which is done by the action of a solenoid valve), as when crossing sharp vertical density gradients, the float is placed in a grounding mode. In this mode, it will not descend to its parking depth to later collect a “full-depth” profile (J.-P. Rannou 2023, personal communication). It is also important to have in mind that the floats’ body and buoyancy engines, as well as the software or firmware used, and the ability to intervene on preset parameters once the drifter is deployed, have greatly evolved during the more than 20 years of the Argo float program. This is, for example, outlined for the ARVOR float type in [André et al. \(2020\)](#), with recent models since the late 2010s not needing any preballasting.

b. Satellite salinity product

Satellite sea surface salinity (SSS) products are used to ascertain when and where low surface salinity (density) occurs. We do not collocate these SSS with missed Argo profiles, as one does not have a measured position for these profiles. Furthermore, the available product does not cover the whole Argo period.

High-resolution (HR) SSS maps based on data from Soil Moisture Ocean Salinity (SMOS) and Soil Moisture Active Passive (SMAP) satellite missions, were developed at the Ocean Salinity Center of Expertise of “Centre Aval de Traitement des Données SMOS” (CATDS CEC-OS) in eight regions ([Boutin et al. 2022](#)). As for other SMOS CATDS CEC products, the HR SSS product uses an optimal interpolation in the time domain, grid node per grid node, simultaneously with the estimation of SSS biases depending on the satellite measurement geometry ([Boutin et al. 2018](#)). The optimal interpolation uses a more tapered smoothing function in order to keep high temporal SMOS and SMAP SSS variability in highly variable regions while filtering outliers in low variability regions. A detailed description is given in the documentation available online (https://data.catds.fr/cecos-locean/Ocean_

[products/HIGH_RESOLUTION_8_REGIONS/documentation/Doc_High_Resolution_8_Regions.pdf](#)).

The use of a more tapered smoothing function allows 1) an improvement of the spatial contrasts either on the SMOS period alone or on the SMOS+SMAP period on almost all considered regional areas and 2) a better restitution of the temporal dynamics for the low SSS at the mouth of river plumes. There is a substantial gain in the correlation indicators with in situ data during the SMOS+SMAP period, as can be seen on the earlier mentioned documentation, and is summarized in the [appendix](#).

HR SSS was produced for 2010–2021 and combines level-2 SMOS and SMAP (after April 2015) data. The merged product has an $\sim 50 \text{ km} \times 50 \text{ km}$ spatial resolution. Instantaneous rain effect on surface salinity was preliminarily removed based on [Supply et al. \(2020\)](#). Although this is arguable for this application of the data, this is not a major contribution here, except maybe at times in the rainier northernmost part of the region investigated, or at its eastern edge north of the equator under the intertropical convergence zone (ITCZ).

The product is noisier before May 2015, when only SMOS data are available. However, even during this SMOS-only period, the random uncertainty that can reach up to 0.5 remains small when compared with the signals of a few units we aim to detect. There is also some degradation of the SSS product (and larger estimated errors) due to radio-frequency interference signals, in particular from sources at Barbados that are large in 2012–14. While this product has been able to better filter these signals than in earlier CEC CATDS products, they remain, but are not a strong hindrance for detecting the very low salinity patches, as Barbados is usually off their path.

The bias correction of the product is local and uses the entire time period of 2010–21 without separating seasons. It is based on a statistical adjustment to a multiyear quantile of the “In Situ Analysis System” (ISAS; [Gaillard et al. 2016](#)) product, with quantiles varying from 50% (median) in regions of low SSS variability to 80% in regions of high SSS variability, as described in [Boutin et al. \(2021\)](#). This adjustment and the land–sea contamination corrections derived at the same time from consistency tests applied to SSS retrieved in various geometries ([Kolodziejczyk et al. 2016](#)) imply that the absolute values are less certain close to the coasts. This is particularly true over the Amazon shelf of South America, impacted by the Amazon plume, which is poorly sampled in the climatology used by ISAS.

An advantage of HR SSS relative to other products such as the CCI+SSS weekly product ([Boutin et al. 2021](#)) is the higher frequencies resolved when there are enough data, as was identified close to the shelf break and in the North Brazil Current (NBC) retroflexion region ([Reverdin et al. 2021](#); [Olivier et al. 2022, 2024](#), manuscript submitted to *Remote Sens. Environ.*). In this region, as currents are large and rapid wind changes induce changes in off-shelf transport of freshwater, SSS changes on time scales of a few days. After combining the different satellite data, which have an average footprint on the order of 43 km, the effective resolution of the product is probably close to $\sim 50 \text{ km} \times 50 \text{ km}$. It implies that thinner low-salinity filaments are smoothed out in this product. On days with data, this product favorably compares to simple mapping of the daily data ([Reverdin et al. 2021](#); [Olivier et al. 2024](#), manuscript submitted

to *Remote Sens. Environ.*). However, there are often data gaps that tend to happen at least one every 2 days, during which the product extrapolates the information. One can thus think of this product as having a 2–3-day resolution (validation and possible uncertainties of HR SSS are presented in the [appendix](#)).

c. OSTIA SST fields

Estimating surface water density requires to combine daily HR SSS with daily sea surface temperature (SST) fields (UNESCO 1983). However, the available daily SST fields present a higher spatial resolution than the SSS fields. There might also be local SST errors on the order of 0.5°C (Donlon et al. 2012). Nonetheless, in this region, the surface water density variability is less dependent on SST than on SSS; thus, as a compromise between time resolution and spatial resolution, we used monthly SST fields instead of the daily ones. This approach captures the effect of the largest spatial SST features on surface density as well as of its seasonal variability. The SST fields used are the foundation SST monthly fields at $0.25^\circ \times 0.25^\circ$ horizontal resolution from the OSTIA product (<https://doi.org/10.48670/moi-00165>) (Donlon et al. 2012; Good et al. 2020).

d. APLUME36

The APLUME36 simulation was designed to investigate the Amazon plume dynamics and SSS variability in the western tropical Atlantic. The numerical model at $1/36^\circ$ resolution in the domain (5°S – 20°N , 70° – 30°W) is the oceanic component of the Nucleus for European Modelling of the Ocean program (NEMO4.2; Madec et al. 2022). It is forced at its meridional boundaries with daily outputs from the MERCATOR global reanalysis GLORYS12 (Lellouche et al. 2021), and at the surface with ERA5 hourly wind speed, atmospheric temperature and humidity, longwave, shortwave radiation, and precipitation. This simulation uses daily and interannual runoff from the “Japanese 55-year Reanalysis” (JRA-55; Suzuki et al. 2018), and includes a tidal forcing. A regional configuration of the NEMO model very similar to the one used here has demonstrated its ability to properly represent the dynamics and properties of the Amazon plume (Ruault et al. 2020). Here, we use daily average salinity fields in the model domain in 2017.

3. Results

a. Missing profiles

We consider two different cases to define a missing profile:

- 1) There are no profile or trajectory data for the whole cycle (i.e., one cycle is missing) and there is no evidence of the float’s presence at the surface (no positioning or attempted transmission).
- 2) There are no profile data or a very incomplete profile (1 or 2 points near the surface, possibly with CTD unpumped) but the float is positioned at the surface and there are trajectory data for the cycle.

There are many reasons for cases 1 or 2 including decoding problems (i.e., incorrect cycle assignment), transmission issues or float programming problems, bottom grounding if the float

remains stuck in the seabed instead of profiling back to the surface, profiling is initiated but the float does not reach the sea surface (sea ice, strong density gradient), or the float may not be able to dive to its parking depth. Sometimes, it is difficult to find the specific reason for a missing profile as this requires an in-depth study of the float’s trajectory and its programming.

Here, we first estimate the proportion of missing profiles corresponding to cases 1 and 2, by float type. We will consider the spatial and temporal distribution of the missing profiles to find whether strong near-surface stratification contributes to the profile losses. To get relevant statistics, we selected a wide swath of the tropical Atlantic (5°S – 15°N , 30° – 80°W), but with a zoom in a more restricted region (0° – 15°N , 59° – 43°W). In case 1, where we do not have a position associated with the missing profile, we linearly interpolate the known adjacent positions to the date of the missing profile (assuming a regular cycle length). To minimize the impact of groundings in our statistics we did not consider missing profiles for which interpolated (case 1) or measured (case 2) position was associated with bathymetry shallower than 1000 m.

1) CASE 1

This is strongly related to the model of floats. In the zoomed region, APEX (Argo float type numbers: 845 and 846), SOLO (851 and 852), and ALTO (as well as Deep SOLO) (873) have the highest percentage of missed profiles (on the order of 6%–7%), followed by S2A (854) (3.5%). On the other hand, it hardly happened for ARVOR and PROVOR floats. In the case of S2A floats, the missed profiles are from a few floats regularly missing profiles (e.g., every 5 cycles). This does not seem to be usually related with particularly strong near-surface stratification, and they will not be further investigated. For the ALTO floats, this is associated with a single float, and this will not be further considered. However, for the APEX and SOLO float types, missed profiles are common and will now be commented upon.

The percentage of profiles missed is computed on a $1^\circ \times 1^\circ$ latitude \times longitude grid, grouping APEX and SOLO floats, and plotted only for grid points with more than 10 profiles (Fig. 1a). These statistics are noisy because they are usually based on a small number of profiles. The figure indicates an area of large percentage values ($>5\%$) of missing profiles west of 45°W and east of 59°W , peaking in its southern part near 4° – 9°N (often $>15\%$; notice that the statistics are not established on the continental shelf) and with a more scattered presence of missing profiles farther east in the 4° – 10°N band. The spatially averaged statistics within the red-outlined box in Fig. 1a (Fig. 1b) indicate a strong seasonal cycle from close to 0% in January–February to a 11%–12% June–August peak. The spatial distribution changes during the seasonal cycle is illustrated by presenting two contrasted seasons, based on the surface salinity seasonal cycle (Figs. 1e,f). In January–June (Fig. 1c), missing profiles (mostly in May–June) are found mostly north of 9°N and west of 50°W , whereas in July–December (Fig. 1d), there are still missing profiles (mostly July–October) in this region, but also between 5° and 9°N west of 42°W , and extending farther east with lesser concentrations in the 4° – 10°N latitude band. There are other scattered local loss maxima, such

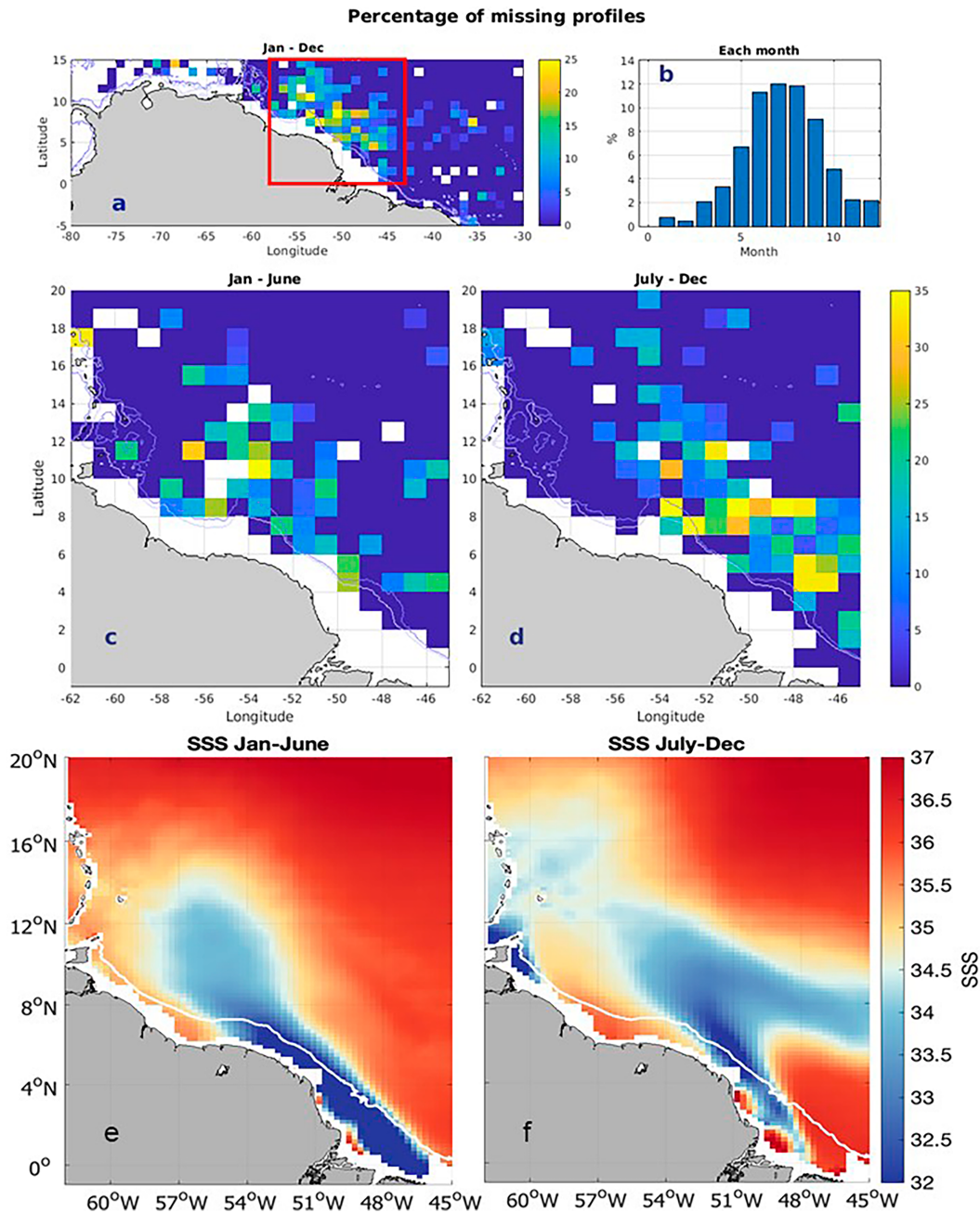


FIG. 1. Percentage of missing profiles of SOLO and APEX floats: (a) annual average distribution in $1^\circ \times 1^\circ$ boxes; (b) seasonal cycle of the proportion of missing profiles in the red-outlined box of (a); (c),(d) the percentage of missing profiles of SOLO and APEX floats for two 6-month seasons; and (e),(f) the average HR SSS for those two seasons (the 100-m bathymetry contour is overlaid in white).

as near $15^\circ\text{--}17^\circ\text{N}/67^\circ\text{--}70^\circ\text{W}$, which might be due to possible grounding nearby, as well as near 4°N related to one float with anomalous missing profiles, but no indication of low surface salinity.

The average HR SSS for the two corresponding seasons presented in Figs. 1e and 1f presents a pattern of low surface salinity roughly corresponding to the higher frequencies of missed profiles. The spatial and temporal distributions of the

missing profiles for APEX and SOLO floats suggest that missing a profile could be linked to the presence of strong near-surface stratification that either prevents the float to reach the surface or delays the time when the float reaches the surface and thus the float does not spend enough time at the sea surface to transmit a profile (many of these floats used the Argos transmission system, which required a long surface time to allow for the data transmission).

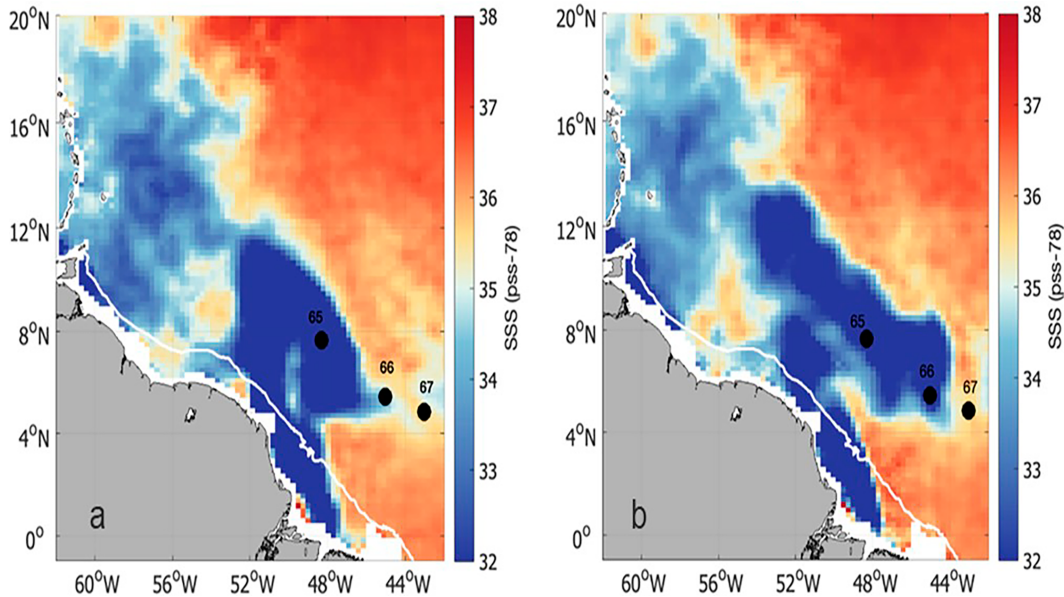


FIG. 2. HR SSS on (a) 19 and (b) 29 Jul 2021 with the black dots for three very limited profiles of ARVOR float 6900892 profiles; 29 Jul [in (b)] corresponds to the date when profile 66 is transmitted. The interrupted descent for profile 66 happened earlier just after the previous profiles on 19 Jul [in (a)] close to the position of station 65. On 29 Jul, the Argo float surface data were SSS = 30.81 and SST = 29.04°C with colocalized satellite salinity of 29.57 [cycles 65 with transmission due on 19 Jul and 67 with transmission due on 8 Aug, after a failed descent on 29 Jul [in (b)] close to the position of profile 66 were also strongly affected by the fresh surface water].

2) CASE 2

For SOLO floats in the zoomed region, 6% of the profiles are missing but the float is positioned while at the surface and some data are transmitted. It is hazardous to speculate on the reason for the lack of profile, but most profiles are missing at the end of the float's life. These missing profiles are distributed almost evenly both geographically (5°S–15°N, 30°–80°W) and seasonally. Because there is no hint that the missing profiles are related to strong near-surface stratification, those cases are not further considered. However, there are also instances for ARVOR or PROVOR floats (altogether 2.6% of all the ARVOR/PROVOR profiles in the June–August season with the lowest salinities) when the float started a descent, which was later aborted because of the bottom detection algorithm and which are often associated with very fresh surface lenses. We illustrate this for float 6900892, during its drift in the North Equatorial Countercurrent (NECC) after a freshwater lens had separated from the NBC retroflection in early to mid-July 2021 (Fig. 2). This float already had difficulty descending during cycle 64 (with $S = 32.818$ at 8 m), requiring 29 pump actions, whereas the next three profiles were aborted during descent. For example, for cycle 66, the trajectory data indicate that the float made several attempts to descend on 19 July 2021 but the descent aborted at 9–10 dbar due to the grounding detection algorithm. This descent was actually tried just after transmission of profile 65 with $S = 30.814$ at 12 dbar. Then the float started its 10-day drift at pressures between 9 and 0 dbar. The “profile” point made about 10 days later started at 0.3 dbar, which was too shallow for pumping water

through the CTD; thus, salinity data are flagged as being bad. When collocating these missed descents (cycles 65, 66, 67) with the HR SSS products at the time of the previous profile transmission (from 9 to 29 July 2021), we find that in all instances the float tried to descend in freshwater advected in the NECC, east of the NBC retroflection, close to the southeastern border of the freshwater tongue (example of Fig. 2).

b. Statistics of low surface salinity or density distribution

At each grid point of the satellite SSS product or the estimated density, we computed the frequency of daily salinity (alternatively density) below different thresholds for the period January 2010–November 2021. We averaged those for each calendar month in the red-outlined box of Fig. 1a in order to get an annual cycle of the frequency of low salinity (density). A very strong seasonal cycle is found for all salinity or density thresholds (Fig. 3). For the 32.5 salinity threshold, the maximum frequency happens in June–August (Fig. 3b) with transition seasons in February–April and October–December. When instead considering surface density (with the caveat that this is based on daily SSS, but monthly SST) (Figs. 3d–f), we find a small shift (roughly by 1 month) relative to the seasonal cycle in Figs. 3a–c that is accountable to the seasonal cycle of SST. Nonetheless, and as expected for this region, it is salinity that dominates the occurrence of low surface density. There is also a small tendency for the seasonal cycle to shift later when the salinity (density) threshold is set higher (but by less than a month).

The frequency maps of daily HR SSS lower than the thresholds [similar maps for surface density (not shown)] mimic the ones of average salinity (Figs. 1e,f) with a strongly varying

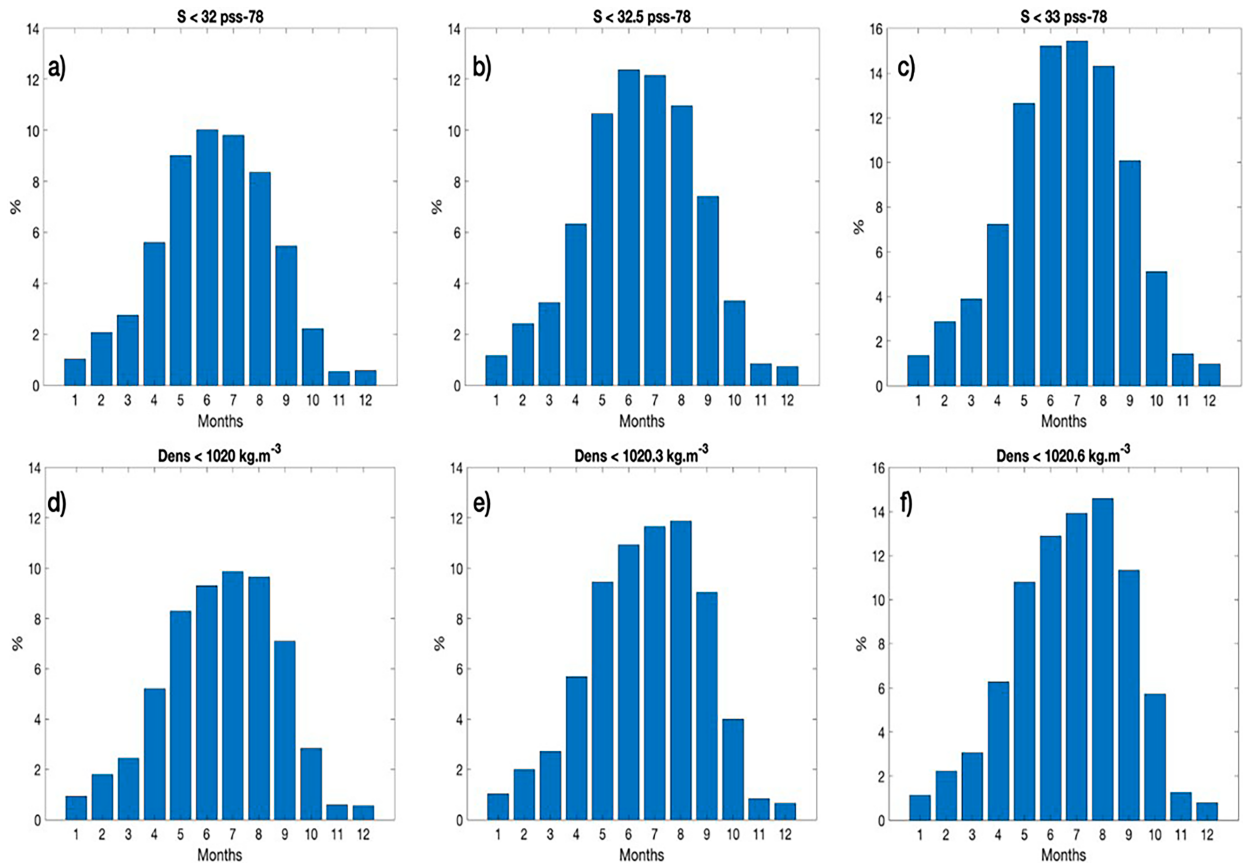


FIG. 3. Frequency of daily gridded HR SSS less than a salinity threshold averaged in the red-outlined box of Fig. 1a for (a) $S < 32$, (b) $S < 32.5$, and (c) $S < 33$. Also shown is frequency of surface densities less than a density threshold in the red-outlined box of Fig. 1a for (d) 1020, (e) 1020.3, and (f) 1020.6 kg m^{-3} (note that the estimated density fields are daily, based on the daily HR SSS, but combined with monthly OSTIA SSTs).

seasonal pattern (two seasons in Fig. 4 for $SSS < 32.5$). The pattern in the first part of the year (mostly May–June) presents a maximum frequency band located on the shelf north of 4°N , extending off the shelf in a northwestward/northward direction west of 51°W over the Demerara Rise, and toward 12°N , 57°W . In the second part of the year, the largest frequencies north of 4°N are off the shelf near 51° – 54°W (east of the Demerara Rise) extending to 10°N , and mostly then turning clockwise following the retroreflection of the NBC in the NECC. There is also a less pronounced tongue of high frequency extending from the retroflexion toward the northwest (Fig. 4). This freshwater path was discussed in Olivier et al. (2024, manuscript submitted to *Remote Sens. Environ.*). It corresponds to Ekman transports of freshwater patches first geostrophically advected to the northwest of the NBC retroflexion, in particular by NBC rings. This was particularly pronounced in the late summer of 2021, and is strongly variable interannually.

4. Discussion

Similarities in the seasonal cycle of the frequency of missing profiles (Fig. 1b) with the ones of low salinity or low density (Fig. 3) are strongly suggestive that the missing profiles (at

least the ascending ones of case 1) are largely associated with the very low density of the freshest surface waters. The best agreement in the seasonal cycle is between Figs. 1b and 3e. It is thus tempting to roughly attribute this to a threshold of surface salinity or density for this region of 32.5 or 1020.3 kg m^{-3} , respectively, under which SOLO and APEX floats could not profile to the surface or at least not in time for data transmission (the salinity/density threshold might be a little lower for SOLO than for APEX floats). The spatial patterns of missing profiles (Figs. 1c,d) also bear similarities with the ones of the frequency of salinity below a set threshold of 32.5 (Fig. 4). This is however less reliable, because of the small number of floats and profiles at each grid point and thus the noisy pattern on the maps. Also, part of the differences may arise from the longer period for the Argo floats statistics, which only partially overlaps the one for the satellite salinity product.

Even in this region with large surface salinity variability, we found that SST variability also contributes to the variability in surface stratification with respect to the deep ocean. However, we have only partially taken it into account in the estimation of surface density, as we used monthly OSTIA SST products. It would be interesting to use daily SST maps, even though their different resolution when compared with HR SSS, and of errors on

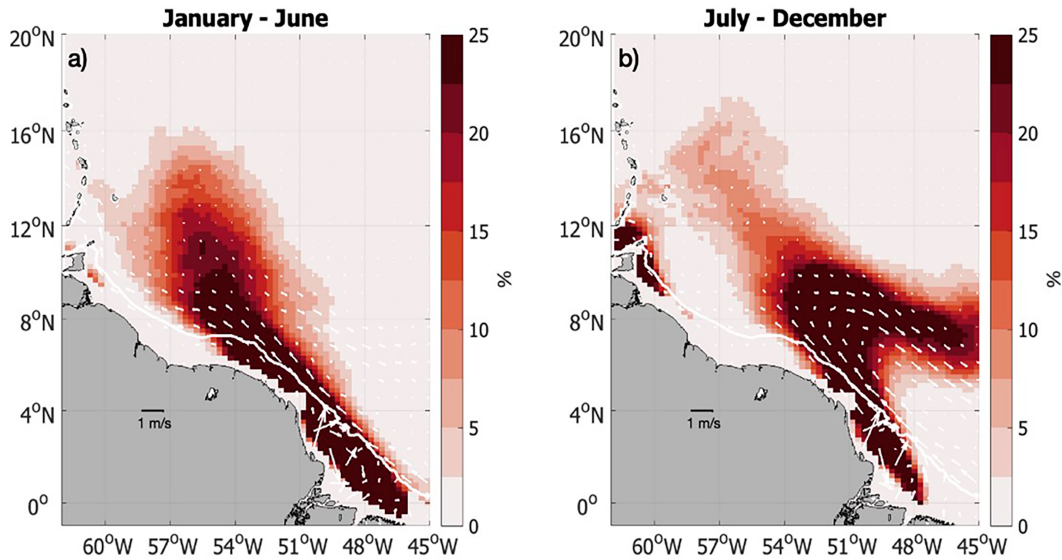


FIG. 4. Frequency of satellite salinity below the salinity threshold 32.5 for (a) January–June and (b) July–December. Average geostrophic currents for the two seasons in 2010–21 are overlaid (in white).

SST and SSS might limit the validity of what is estimated. We nonetheless expect the daily mesoscale SST signals to have a small contribution on surface density, albeit, off the shelves there is a tendency for higher temperatures to be associated with the lowest salinities (Reverdin et al. 2021; Olivier et al. 2022).

The above comparisons strongly suggest that APEX floats and, to a lesser extent, SOLO floats were not capable of ascending across the large salinity/density gradients near the sea surface, when surface salinity was as low or lower than 32.5. This is supported by overall statistics on uppermost salinities in profiles of the different types of Argo floats (Table 1; Fig. 5). The percentage number for June–August in S2A is close to the one for satellite salinity distribution (orange curve in Fig. 5), albeit a little smaller, even for the very low surface salinity. It is possible that in particularly low surface density cases, even S2A profiles are not complete near the surface, as happened for three profiles in a particularly strong fresh pool in September 2021 (S. Wijffels 2023, personal communication). Neglecting these very rare cases and retaining S2A as the norm, we find that

all other float types have significantly less occurrences of low uppermost salinity, and for SOLO and APEX float types, this is the case even if accepting all QCs. The extreme case is for APEX floats with no occurrence of uppermost salinities smaller than 32, and still a very small occurrence for a threshold at 33. As discussed earlier there is also an issue of misdiagnosed grounding during descent with very low surface salinity water for ARVOR/PROVOR floats (2.6% in June–August), which contributes to the differences with S2A statistics in Table 1. There is also the possibility that bad or probably bad flags on surface data were not correctly applied in the presence of very low surface salinity (for SOLO, S2A, and ARVOR/PROVOR floats). This surface flagging issue affects only a small number of profiles and has much less effect. In addition to the missing profiles, another contribution to the lower frequency of low uppermost salinity data relative to HR SSS for SOLO, APEX, and for early ARVOR/PROVOR floats is that the uppermost depth of the salinity profile was fairly deep (5–7 m from the surface); thus, their uppermost salinity is likely higher than at the surface.

TABLE 1. June–August frequency of uppermost salinity (pump on) less than different salinity thresholds for different types of Argo floats in the red-outlined rectangular region (Fig. 1a). Profiles with more than 25% of salinity qc data larger than 2 (bad or probably bad) have been removed from the count. For each type of profiler, the left column is when the uppermost salinity has $qc \leq 2$ (thus, including “not known, good, or probably good” data), and the right column is for all qc. Normalization is with total number of profiles for the given type of profiler, thus for all qc of uppermost salinity.

	S2A		ARVOR		APEX		SOLO	
	$qc \leq 2$	all qc	$qc \leq 2$	all qc	$qc \leq 2$	all qc	$qc \leq 2$	all qc
$S < 30$	2.2	2.2	0.6	0.7	0	0	0	0
$S < 31$	4.6	4.6	1.5	1.6	0	0	0.2	0.2
$S < 32$	8.4	8.4	5.3	5.4	0	0	1.8	1.8
$S < 33$	15.2	15.3	12.3	12.4	0.7	0.7	5.9	6.3
$S < 34$	24.6	24.7	22.1	22.5	3.3	3.3	10.2	11.2
$S < 35$	34.9	35.0	34.5	35.0	15.7	15.7	19.8	21.2

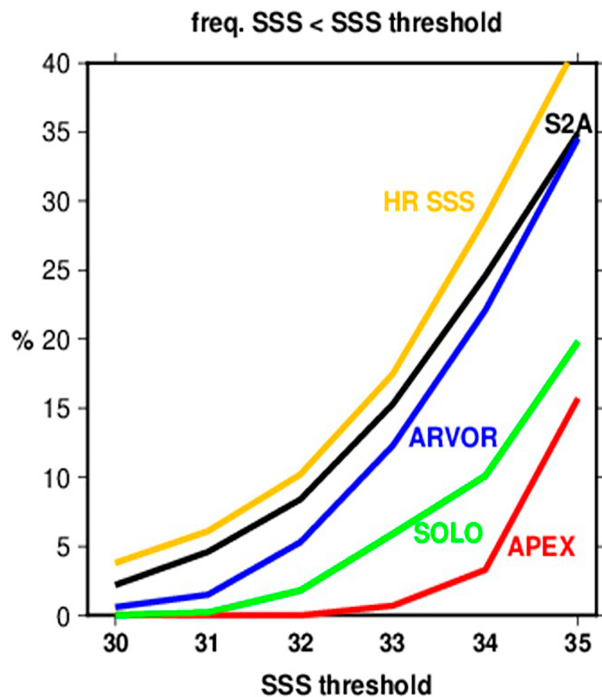


FIG. 5. June–August frequency of uppermost salinity (pump on) less than salinity thresholds (horizontal axis) for different types of Argo floats [ARVOR (blue), SOLO (green), APEX (red), and S2A (black)] and for satellite HR SSS (orange), in the red-outlined rectangular region in Fig. 1a. Argo profiles with more than 25% of salinity data with QC larger than 2 (bad or probably bad) have been removed from the count, as well as all profiles for which the SSS QC was larger than 2. Satellite salinity grid points on the shelf have been removed.

These different characteristics contribute to underrepresenting low surface salinities in the Argo database. This will be particularly pronounced in the early period of Argo deployments, when there was a high proportion of SOLO and APEX floats. S2A floats became more prominent starting in 2013, and after 2018, there is no more SOLO floats, and very few APEX floats. Thus, after 2018, most floats have a high

vertical resolution near the surface, measure (pump on) closer to the surface, and their surface salinities are less likely to have been flagged as not good.

We provide an estimate of the bias in average monthly surface salinity resulting from not sampling low salinities smaller than 32.5 as found for the APEX and SOLO floats, by simulating it in the nearly 11-yr-long set of daily satellite salinity fields (Fig. 6). With this choice, we obtain for the annual average (Figs. 6a,b) a difference (Fig. 6b) in the extended Amazon plume, which often exceeds 1. Not surprisingly, the effect is much larger for the season June–August (not shown), where the occurrence of the freshest waters is largest (Fig. 3). This also implies that the seasonal cycle of SSS products based on Argo floats SSS would be underestimated, in particular for the early period of the Argo float deployments, when there were more SOLO and APEX floats (although altogether less floats drifted in this area during that period than more recently since 2013). It is thus very possible for the period before 2013 that the biases in the in situ–based products such as ISAS result in an underestimation of the seasonal cycle of surface salinity in the Amazon plume by 20%–30%. On the other hand, in the most recent years (since 2019, in particular), this underestimation of the amplitude of the seasonal cycle should be much smaller in the Argo-based products, with a much smaller positive salinity bias. It could still be present, for example, because of the loss of profiles in nondescending ARVOR floats.

Because of the change in the models of Argo floats and modes of operation near the surface (Fig. 7 illustrates the rates of missed profiles each year), this will also contribute to trends in in situ surface salinity products. For example, if the transition is from full effect of the missing profiles in 2010 at the beginning of the salinity satellite area toward no effect recently, there would be a negative trend corresponding to the difference map (Fig. 6c) interpreted as units per decade, with the largest effect in the freshest season June–August and the weakest effect in January–March. There is some indication that this is the case (Fournier and Lee 2021). However, as even in 2010, there was already a mix of float types, and there are still a few missing profiles recently, the overall trend in in situ surface salinity products might be smaller. It is interesting to notice that Argo floats

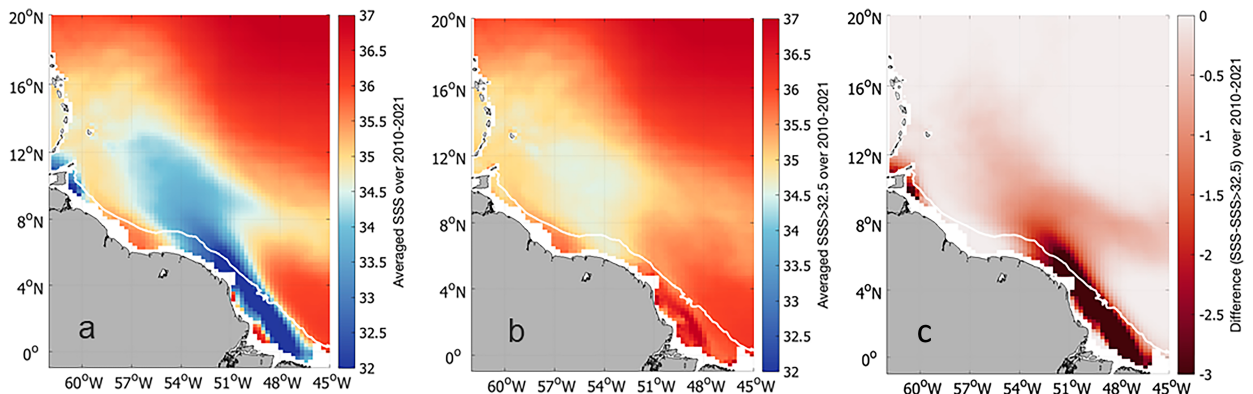


FIG. 6. January 2010–November 2021 HR SSS salinity: (a) average salinity, (b) average salinity but including at each grid point only the days with salinity larger than the threshold 32.5, and (c) the difference (a) minus (b).

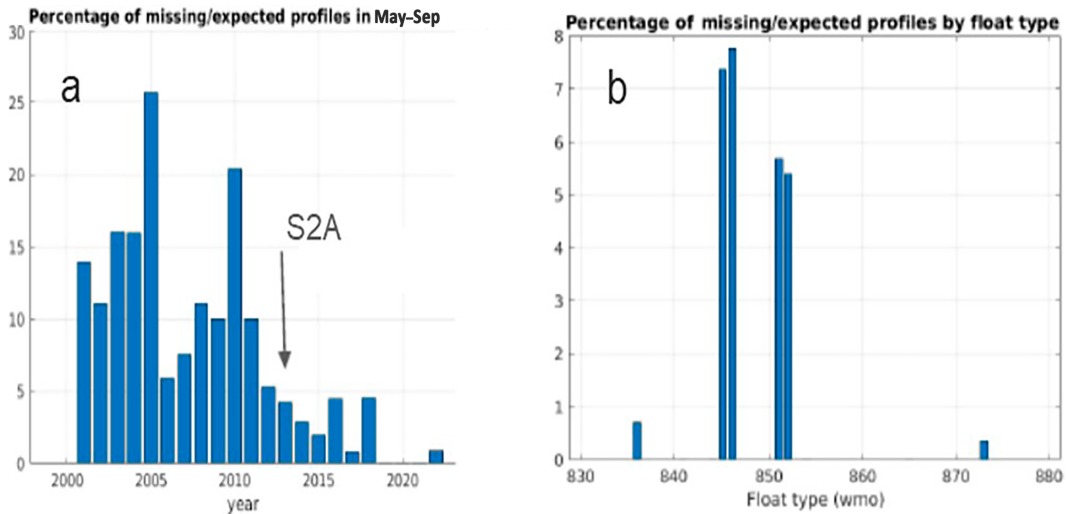


FIG. 7. (a) Time distribution by year of missing profiles due to stratification during May–September, and (b) percentage for each float type during the whole period (red-outlined box of Fig. 2); 2016 and 2018 were the last years with APEX and SOLO floats [in (b): 845–846 for APEX floats and 851–852 for SOLO floats], and the arrow on (a) indicates when S2A floats start providing the majority of profiles.

might have missed interannual variability in this region (Grodsky and Carton 2018), which might be partially related to these missing profiles, but also to the random sampling of a very spatially and temporarily variable SSS field by Argo profilers.

We cannot fully separate in these potential biases and trends what would directly result from the history of missing profiles from what is caused by the change in the uppermost depth reported in the profiles. Indeed, the two are probably intertwined. For example, in recent cruise data (Olivier et al. 2024, manuscript submitted to *Remote Sens. Environ.*) and in recent Argo profiles, we find that vertical salinity gradients in the upper 5–7 m are more commonly larger than 1 pss when surface salinity is very low (less than 32.5, for example) than when it is higher. If the early floats did not report profiles in the presence of very low surface salinity (density), as supported by this study, they might also have missed most of the instances with very large vertical salinity gradients. Of course, the results will be different in regions with less extreme low surface salinity or other sources of freshwater.

The missing profiles with low SSS in the Argo set will affect the results of optimal interpolation of Argo SSS such as is done in the ISAS fields, but the effect will depend on the proportion of missing profiles and on how much the incorporated Argo profiles modify the guess climatology. This is of course compounded with the lack of Argo data above 5-m depth in the early part of the Argo program, and the way subsurface data information is extrapolated to the surface in the ISAS product (when no data are available in a profile in the upper 5 m, it is the value between 5 and 10 m that is retained, thus likely further overestimating surface salinity).

In this discussion, we have considered the product HR SSS as ground truth. However, it is possible that the adjustment to positively biased ISAS salinity fields influences the

reported HR SSS values, although not to a large degree off the shelves (cf. appendix). The HR SSS product might also not reproduce the lowest observed salinities due to its effective spatial resolution of 50 km and the temporal resolution of a couple of days that will smear the smallest scales of salinity variability.

5. Conclusions

We have found clear evidence that technological constraints for early Argo floats that limited either ascent or descent through large salinity/density gradients have resulted in a significant loss of profile data in the Amazon plume area, specifically targeting the lowest surface salinity (in particular, for surface salinity smaller than 32.5). We also noticed in the Argo data, a small percentage (less than 1% in ARVOR/PROVOR and SOLO floats) when low salinity at the surface was flagged, which is suspicious but difficult to further investigate. Although this percentage is small, this corresponds to very small salinities that might be of particular interest.

Altogether, in the very low salinity areas ($S < 32.5$) probably half the profiles have been missed. This was particularly the case for APEX and SOLO type floats that did not ascend to the surface but is also present to a lesser extent on ARVOR/PROVOR floats because of aborted descents. Thus, the losses have been largest in the early years of the program, less important since 2013, and smallest after 2018. Although variations of surface density are largely constrained in this area by variations of surface salinity, there are contrasts in eddy structure and seasonal variability in surface temperature that slightly compound the salinity effect to lower surface density. In particular, during fall the higher temperatures contribute to lower density, thus further profile loss, which could explain

the higher profile loss rate in the fall than in the spring, contrary to what is seen in the satellite SSS statistics. There is also a possible contribution of temperature mesoscale variability, not included here, which further contributes to lower surface density in low salinity patches.

This study is a first step to evaluate whether and where Argo profile loss impacts the monitoring of the freshwater content in the upper ocean, as well as the validation and evaluation of surface salinity products, such as produced by ocean reanalyses or satellite-based products that rely on the available in situ Argo data. One important question that will need to be later addressed is whether a selective loss of profiles in regions of low-density surface waters (and large density contrast with the deeper ocean) documented for APEX and SOLO floats happened elsewhere. Although this is anecdotal, there also seems to be more missing profiles in the equatorial Atlantic east of 45°W between 4° and 10°N during July–December (4°–10°N). This suggests that this phenomenon might also be happening in other areas of the tropical Atlantic with low surface salinity (density), for example, associated to the west African river plumes. Early on in the Argo program, there were also APEX floats that could not ascend to the surface in the warm (less dense) summer surface layer of the western subtropical North Pacific (S. Riser 2022, personal communication), and there are such cases with SOLO floats not reaching the sea surface in the subtropical South Pacific (J. Gilson 2023, personal communication; for example, float 3901123 between 2012 and 2020). There were also APEX floats deployed in the Beaufort Gyre of the Arctic Ocean that did not return to the surface in the presence of a very fresh surface layer (J. Morrison 2022, personal communication). We can thus expect that profile loss has happened in various regions with very low surface density, such as other low surface density river plumes, the vicinity of the intertropical convergence zone, and in particularly strong fresh surface waters, such as observed in the equatorial Pacific during the SPURS-2 campaign (Lyer and Drushka 2021). It probably also happened at high latitudes, in situations with extreme surface freshening from sea ice melt or other fresh surface water sources.

Acknowledgments. Support was obtained by the JPI-Ocean Project EUREC4A-OA, as well as from TOSCA SMOS-Ocean and Centre Aval de Traitement des Données SMOS (CATDS) projects of the French National Centre for Space Studies, and by SNO Argo-France. Comments by Annie Wong, Steve Riser, John Gilson, and Jean-Philippe Rannou, as well as from three anonymous reviewers, were very much appreciated. Computing facilities to produce APLUME36 were provided by GENCI Project GEN7298. This work received funding from the French INSU/LEFE program through the LEFE-GMMC Mad-Strat project.

Data availability statement. CATDS SSS are available at the CATDS Production Data Center (CPDC) (<https://www.catds.fr>). Argo data are available at the ARGO GDAC hosted by Coriolis (Brest, France; <http://www.coriolis.eu.org>;

<https://doi.org/10.17882/42182>). OSTIA dataset (<https://doi.org/10.48670/moi-00165>) accessed on 6 January 2023 online (https://data.marine.copernicus.eu/product/SST_GLO_SST_L4_NRT_OBSERVATIONS_010_001/description). The daily geostrophic currents from altimeter satellite gridded sea level anomalies (DUACS processing system) were obtained on 12 January online (<https://doi.org/10.48670/moi-00148>).

APPENDIX

Satellite Salinity Product Validation

The validation of the HR SSS product is done by comparing it with Argo float profiles' uppermost pumped salinity (often near 5 m, but in recent years there has been an increase in data closer to the surface near 1- or 2-m depth), as well as with validated thermosalinograph data from ships of opportunity. The Argo floats are distributed throughout the region, except over the South American shelves where data coverage is very poor [a region where the product is thus not validated, and for which there is the same lack of data in the in situ-based products, such as ISAS (Gaillard et al. 2016) used to adjust the climatological long-term averaged SSS].

The statistical comparison with in situ data is summarized in Fig. A1 (for the exponential core). The overall dispersion (robust std difference) variability only is 0.58 for the joint SMOS–SMAP period, with part associated with low salinity in in situ data often corresponding to higher salinities in the mapped product. This is surprising as both the Argo float upper measurements and TSG data are often deeper than 4 m

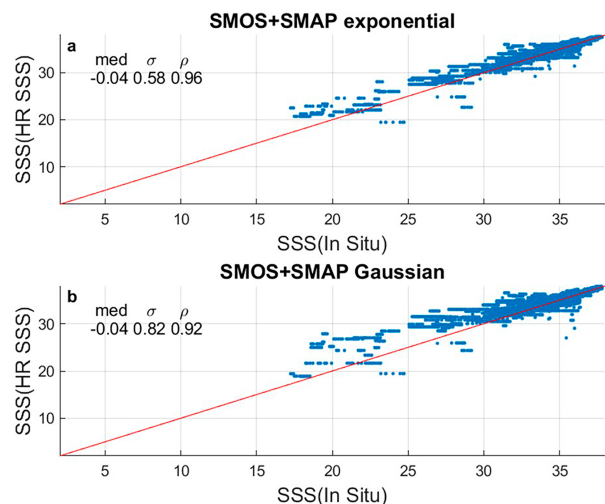


FIG. A1. Validation of HR SSS product during the SMOS+SMAP (April 2015–November 2021) period [(a) exponential kernel as used here; (b) Gaussian kernel]. A comparison is shown with all the individual collocated data from the Pi-MEP validated database, which includes all Argo floats' uppermost pumped data with QC less than 2, except for gray-listed floats, as well as data from quality-controlled thermosalinographs (ships on a line from French Guyana to Europe from SNO SSS delayed-mode database). The statistics provided are for the median, robust standard deviation of the differences σ , and correlation coefficient between satellite and in situ SSS ρ .

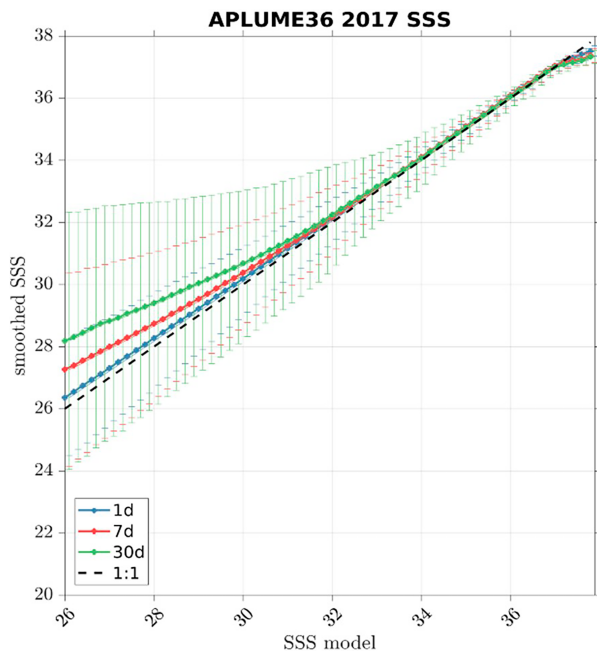


FIG. A2. Comparison of measured salinity at satellite-product resolution with gridpoint salinity in the APLUME36 model simulation in 2017 in the whole western Atlantic domain (5°S – 20°N , 70° – 30°W). The satellite-product resolution was simulated by averaging model salinity over a 60-km radius and over 1 day (blue), 7 days (red), and 30 days (green). The satellite-product resolution data were sorted as a function of gridpoint model salinity by 0.1 salinity class; the vertical bars correspond to the standard deviation of the averaged salinity within these salinity classes.

below the surface, thus probably with a higher salinity than in the top 1 cm near the surface that the satellite salinity senses.

However, there are different possibilities for such differences. For example, this could be due to the lowest Argo salinities being in small time–space structures not reproduced by the $\sim 50\text{ km} \times 50\text{ km}$ -resolution product. It could also result from the adjustment of the SSS fields to a reference SSS field over the whole period, with positive biases in the reference field.

For this satellite salinity product, the ISAS fields are used to provide an overall adjustment, as a gridpoint based correction. In regions that are highly variable, such as in the northwestern tropical Atlantic where the fresh waters of the Amazon plume spread, the adjustment is by adjusting the 80% highest percentiles in the satellite salinity product time series to the 80th highest percentile in ISAS. Assessing whether this percentile is affected by the undersampling of low salinity in situ situations (missed Argo profiles) in ISAS and by how much is difficult. Except on the shelves between the river’s mouth and 5°N , one can presume that this 80% highest percentile is likely to correspond mostly to the season when profiles with SSS lower than 32.5 are absent, and thus the adjustment to ISAS might not be affected by the missing profile issue discussed in this paper. On the other hand, on the shelf areas close to the river’s mouth, which are very poorly sampled by Argo floats and other in situ data in this region, the ISAS product might not be an appropriate reference to adjust

the satellite salinity products. Furthermore, on the shelves, the satellite salinity product has other issues due to possible land contamination.

Another possible reason for higher salinity in the HR SSS product at the lowest observed in situ salinity data is the resolution of the product, which is on the order of 50 km and which does not resolve the smallest structures. The interpolation in time between successive satellite passes with about one satellite pass every day could also smooth out the freshest surface structures. When there is a good satellite coverage in a day, as is found in half the days during the joint SMAP–SMOS area (since May 2015, except for one short interruption in the SMAP data), we found that the product is close to the satellite data in that day processed as in Reverdin et al. (2021) and Olivier et al. (2024, manuscript submitted to *Remote Sens. Environ.*). A recent high-resolution model simulation (APLUME36 simulation) is used to evaluate the impact of the satellite footprint and the time average involved in the gridded surface salinity product. For that, the modeled instantaneous gridpoint salinities are considered as the “real” salinity data, and they are compared with an averaged version of the simulated salinities to a spatial resolution of 60 km, and temporal resolutions of 1, 7, and 30 days. The comparison is sorted as a function of the “real salinity” and presented averaged in this region (Fig. A2). In all cases, this results in a bias, where for the lowest “real” salinity data (less than 32), the model simulated salinity is higher with a salinity bias that reached 1 at $S = 26$ for weekly data. On the other hand, for a 1-day average, which is less than what we think the satellite product represents, the bias is much smaller but still positive in this simulation in the 26–32 salinity range.

REFERENCES

- Anderson, J. E., and S. C. Riser, 2014: Near-surface variability of temperature and salinity in the tropical and subtropical ocean: Observations from profiling floats. *J. Geophys. Res. Oceans*, **119**, 7433–7488, <https://doi.org/10.1002/2014JC010112>.
- André, X., and Coauthors, 2020: Preparing the new phase of Argo: Technological developments on profiling floats in the NAOS project. *Front. Mar. Sci.*, **7**, 577446, <https://doi.org/10.3389/fmars.2020.577446>.
- Böhme, L., and U. Send, 2005: Objective analyses of hydrographic data for referencing profiling float salinities in highly variable environments. *Deep-Sea Res. II*, **52**, 651–664, <https://doi.org/10.1016/j.dsr2.2004.12.014>.
- Boutin, J., and Coauthors, 2016: Satellite and in situ salinity: Understanding near-surface stratification and sub-footprint variability. *Bull. Amer. Meteor. Soc.*, **97**, 1391–1407, <https://doi.org/10.1175/BAMS-D-15-00032.1>.
- , and Coauthors, 2018: New SMOS sea surface salinity with reduced systematic errors and improved variability. *Remote Sens. Environ.*, **214**, 115–134, <https://doi.org/10.1016/j.rse.2018.05.022>.
- , and Coauthors, 2021: Satellite-based sea surface salinity designed for ocean and climate studies. *J. Geophys. Res. Oceans*, **126**, e2021JC017676, <https://doi.org/10.1029/2021JC017676>.
- , J.-L. Vergely, L. Olivier, G. Reverdin, X. Perrot, and C. Thouvenin-Masson, 2022: SMOS SMAP high resolution SSS maps in regions of high variability, generated by CATDS CEC. SEANOE, accessed 10 January 2023, <https://doi.org/10.17882/90082>.

- Cabanes, C., V. Thierry, and C. Lagadec, 2016: Improvement of bias detection in Argo float conductivity sensors and its application in the North Atlantic. *Deep-Sea Res. I*, **114**, 128–136, <https://doi.org/10.1016/j.dsr.2016.05.007>.
- Coles, V. J., M. T. Brooks, J. Hopkins, M. R. Stukel, P. L. Yager, and R. R. Hood, 2013: The pathways and properties of the Amazon River plume in the tropical North Atlantic Ocean. *J. Geophys. Res. Oceans*, **118**, 6894–6913, <https://doi.org/10.1002/2013JC008981>.
- Donlon, C. J., M. Martin, J. Stark, J. Roberts-Jones, E. Fiedler, and W. Wimer, 2012: The Operational Sea Surface Temperature and Sea Ice Analysis (OSTIA) system. *Remote Sens. Environ.*, **116**, 140–158, <https://doi.org/10.1016/j.rse.2010.10.017>.
- Drucker, R., and S. C. Riser, 2014: Validation of Aquarius sea surface salinity with Argo: Analysis of error due to depth of measurement and vertical salinity stratification. *J. Geophys. Res. Oceans*, **119**, 4626–4637, <https://doi.org/10.1002/2014JC010045>.
- Fournier, S., and T. Lee, 2021: Seasonal and interannual variability of sea surface salinity near major river mouths of the World Ocean inferred from gridded satellite and in-situ salinity products. *Remote Sens.*, **13**, 728, <https://doi.org/10.3390/rs13040728>.
- Gaillard, F., T. Reynaud, V. Thierry, N. Kolodziejczyk, and K. von Schuckmann, 2016: In situ-based reanalysis of the global ocean temperature and salinity with ISAS: Variability of the heat content and steric height. *J. Climate*, **29**, 1305–1323, <https://doi.org/10.1175/JCLI-D-15-0028.1>.
- Good, S. A., M. J. Martin, and N. A. Rayner, 2013: EN4: Quality-controlled ocean temperature and salinity profiles and monthly objective analyses with uncertainty estimates. *J. Geophys. Res. Oceans*, **118**, 6704–6716, <https://doi.org/10.1002/2013JC009067>.
- , and Coauthors, 2020: The current configuration of the OSTIA system for operational production of foundation sea surface temperature and ice concentration analyses. *Remote Sens.*, **12**, 720, <https://doi.org/10.3390/rs12040720>.
- Grodsky, S. A., and J. A. Carton, 2018: Delayed and quasi-synchronous response of tropical Atlantic surface salinity to rainfall. *J. Geophys. Res. Oceans*, **123**, 5971–5985, <https://doi.org/10.1029/2018JC013915>.
- Ishii, M., M. Kimoto, K. Sakamoto, and S.-I. Iwasaki, 2006: Steric sea level changes estimated from historical ocean subsurface temperature and salinity analyses. *J. Oceanogr.*, **62**, 155–170, <https://doi.org/10.1007/s10872-006-0041-y>.
- Kolodziejczyk, N., J. Boutin, J.-L. Vergely, S. Marchand, N. Martin, and G. Reverdin, 2016: Mitigation of systematic errors in SMOS sea surface salinity. *Remote Sens. Environ.*, **180**, 164–177, <https://doi.org/10.1016/j.rse.2016.02.061>.
- Lellouche, J.-M., and Coauthors, 2021: The Copernicus global 1/12 oceanic and sea ice GLORYS12 reanalysis. *Front. Earth Sci.*, **9**, 698876, <https://doi.org/10.3389/feart.2021.698876>.
- Le Traon, P. Y., 2013: From satellite altimetry to Argo and operational oceanography: Three revolutions in oceanography. *Ocean Sci.*, **9**, 901–915, <https://doi.org/10.5194/os-9-901-2013>.
- Llovel, W., S. Purkey, B. Meyssignac, A. Blazquez, N. Kolodziejczyk, and J. Bamber, 2019: Global ocean freshening, ocean mass increase and global mean sea level rise over 2005–2015. *Sci. Rep.*, **9**, 17717, <https://doi.org/10.1038/s41598-019-54239-2>.
- Lyer, S., and K. Drushka, 2021: The influence of pre-existing stratification and tropical rain modes on the mixed layer salinity response to rainfall. *J. Geophys. Res. Oceans*, **126**, e2021JC017574, <https://doi.org/10.1029/2021JC017574>.
- Maded, G., and Coauthors, 2022: NEMO ocean engine: Version 4.2. IPSL Climate Modelling Center Scientific Note 27, 323 pp., <https://doi.org/10.5281/zenodo.6334656>.
- Olivier, L., and Coauthors, 2022: Wintertime process study of the North Brazil Current rings reveals the region as a larger sink for CO₂ than expected. *Biogeosciences*, **19**, 2969–2988, <https://doi.org/10.5194/bg-19-2969-2022>.
- Owens, W. B., and A. P. S. Wong, 2009: An improved calibration method for the drift of the conductivity sensor on autonomous CTD profiling floats by θ - S climatology. *Deep-Sea Res. I*, **56**, 450–457, <https://doi.org/10.1016/j.dsr.2008.09.008>.
- Reul, N., S. Saux-Picart, B. Chapron, D. Vandermark, J. Tournadre, and J. Salisbuty, 2009: Demonstration of ocean surface salinity microwave measurements from space using AMSR-E data over the Amazon plume. *Geophys. Res. Lett.*, **36**, L13607, <https://doi.org/10.1029/2009GL038860>.
- Reverdin, G., and Coauthors, 2021: Formation and evolution of a freshwater plume in the northwestern tropical Atlantic in February 2020. *J. Geophys. Res. Oceans*, **126**, e2020JC016981, <https://doi.org/10.1029/2020JC016981>.
- Riser, S. C., D. Swift, and R. Drucker, 2018: Profiling floats in SOCCOM: Technical capabilities for studying the Southern Ocean. *J. Geophys. Res. Oceans*, **123**, 4055–4073, <https://doi.org/10.1002/2017JC013419>.
- Roemmich, D., and J. Gilson, 2009: The 2004–2008 mean and annual cycle of temperature, salinity, and steric height in the global ocean from the Argo program. *Prog. Oceanogr.*, **82**, 81–100, <https://doi.org/10.1016/j.poccean.2009.03.004>.
- , and Coauthors, 2019: On the future of Argo: A global, full-depth, multi-disciplinary array. *Front. Mar. Sci.*, **6**, 439, <https://doi.org/10.3389/fmars.2019.00439>.
- Ruault, V., J. Jouanno, F. Durand, J. Chanut, and R. Benshila, 2020: Role of the tide on the structure of the Amazon plume: A numerical modeling approach. *J. Geophys. Res. Oceans*, **125**, e2019JC015495, <https://doi.org/10.1029/2019JC015495>.
- Supply, A., J. Boutin, G. Reverdin, J.-L. Vergely, and H. Bellenger, 2020: Variability of satellite sea surface salinity under rainfall. *Satellite Precipitation Measurement*, Vol. 2, V. Levizzani et al., Eds., Springer, 1155–1176, https://doi.org/10.1007/978-3-030-35798-6_34.
- Suzuki, T., D. Yamazaki, H. Tsujino, Y. Komuro, H. Nakano, and S. Urakawa, 2018: A dataset of continental river discharge based on JRA-55 for use in a global ocean circulation model. *J. Oceanogr.*, **74**, 421–429, <https://doi.org/10.1007/s10872-017-0458-5>.
- UNESCO, 1981: The Practical Salinity Scale 1978 and the international equation of state of seawater 1980. UNESCO Tech. Paper in Marine Science 36, 25 pp.
- , 1983: Algorithms for computation of fundamental properties of seawater. UNESCO Tech. Paper in Marine Science 44, 53 pp.
- von Shuckmann, K., and Coauthors, 2020: Copernicus Marine Service Ocean State Report, issue 4. *J. Oper. Oceanogr.*, **13**, S1–S172, <https://doi.org/10.1080/1755876X.2020.1785097>.
- Wong, A. P. S., and Coauthors, 2020: Argo data 1999–2019: Two million temperature-salinity profiles and subsurface velocity observations from a global array of profiling floats. *Front. Mar. Sci.*, **7**, 700, <https://doi.org/10.3389/fmars.2020.00700>.